Westinghouse Electric Corporation

Energy Systems

Box 355
Pittsburgh Pennsylvania 15230-0355

DCP/NRC1257
NSD-NRC-98-5571
Docket No.: 52-003

February 13, 1998

Document Control Desk
U.S. Nuclear Regulatory Commission
Washington, DC 20555

ATTENTION: T. R. QUAY

SUBJECT: AP600 RESPONSE TO FSER OPEN ITEMS

Dear Mr. Quay:

Enclosed with this letter are the Westinghouse responses to FSER open items on the AP600. A summary of the enclosed responses is provided in Table 1. Included in the table is the FSER open item number, the associated OITS number, and the status to be designated in the Westinghouse status column of OITS.

The NRC should review the enclosures and inform Westinghouse of the status to be designated in the "NRC Status" column of OITS.

Please contact me on (412) 374-4334 if you have any questions concerning this transmittal.

Brian A. McIntyre, Manager
Advanced Plant Safety and Licensing

jml

Enclosure

cc: W. C. Huffman, NRC (Enclosure)
J. E. Lyons, NRC (Enclosure)
T. J. Kenyon, NRC (Enclosure)
J. M. Sebrosky, NRC (Enclosure)
D. C. Scaletti, NRC (Enclosure)
N. J. Liparulo, Westinghouse (w/o Enclosure)

E004 /

3617a.wpf

Table 1 List of FSER Open Items Included in Letter DCP/NRC1257		
FSER Open Item	**OITS Number**	**Westinghouse status in OITS**
440.747F (R1)	6356	Confirm W
440.769F	6343	Action N
480.1107 (R1)	6376	Action N
720.423F (R1)	6135	Confirm W

Enclosure to Westinghouse
Letter DCP/NRC1257

February 13, 1998

FSER Open Item 440.747F *Revision 1* (OITS #6356)

The staff has reviewed WCAP-14727, "AP600 Scaling and PIRT Closure Report," Rev. 1, including Westinghouse's responses to staff and ACRS questions. The staff has determined that most of the questions have been acceptably addressed. However, the staff has concluded that additional discussion is needed in the report to explain the differences between the "data"-based and "hand calculation"-based values of the "pi" groups in the report. These values often differ by up to an order of magnitude, and use of the "pi" values based on data could give somewhat different results in comparing the response of the test facilities to that of the AP600. The staff understands that the hand-calculated values of the "pi" groups were used to keep the AP600 on a consistent basis with the test facility (since there are no "data" values, aside from nominal geometric parameters) for the actual plant. However, the "hand calculation" method requires the use of simplified models, e.g., two-phase flow and pressure drop, which may not reflect actual facility (or plant) behavior. One of the staff's primary objectives in requesting the "closure" report was to evaluate the actual data produced by the facilities in terms of consistency with the importance (rank) assigned to local and system phenomena in the PIRTs. The staff requests that Westinghouse provide additional discussion of the data-related values of dimensionless groups, both in comparison to the "hand-calculated values" and in relation to the ranking in the PIRTs.

Response:

A comparison evaluation of the "data"-based and "hand calculation"-based values of the "pi" groups in WCAP-14727, Revision 1, has been performed to explain differences that exist between these computed values. This evaluation has been performed for the "pi" groups derived from the following models:

- Single loop top down systems scaling
- Multiple loop top down systems scaling
- Bottom-up component scaling

The results of the evaluation indicate a systematic difference exists between the "data"-based and "hand calculation"-based values for those "pi" groups which contain the core flow rate. These differences are the result of the simplified assumptions used in the models to estimate the core flow rate in the "hand-based" calculations for AP600 and the test facilities. However, since the same methodology was applied to the both the AP600 and the test facilities, the use of the "hand-based" calculations for evaluating the scaling of the test facilities is valid.

Additional arguments regarding the differences between the "data"-based and "hand calculation"-based values have been included in Revision 1 of this response. The added sentences and paragraphs are noted in bold-italic font and are marked in the left margin of the response.

The results of the comparison evaluation is attached to this RAI response. This discussion will be incorporated in Revision 2 to WCAP-14727, "AP600 Scaling and PIRT Closure Report," as Section 3.4, "Comparison of PI Groups Evaluated Using Hand Calculations and Test Data."

WCAP-14727 Revisions:

3.4 COMPARISON OF Π GROUPS EVALUATED USING HAND CALCULATIONS AND TEST DATA

The values of the non-dimension time constants (Π groups) for the top down systems scaling, single loop and multiple loop, and the bottom-up component scaling have been examined for consistency. In particular, the Π groups calculated using hand methodology have been compared with those calculated from test data. All Π groups in which these values differed by more than a factor of two have been tabulated and the probable causes for the differences identified. Agreement of these values within a factor of two is judged to be adequate agreement to confirm consistency between these two methods. These tables and further discussion of the impact on the validity of the test data are provided in the sections below.

3.4.1 Single Loop Scaling

The single loop Π groups for which the hand calculated values differ from the values calculated from test data by more than a factor of 2 are tabulated in Table 3.4-1. There are 19 Π groups where this difference appears. Most of the differences are in the range of 2.2 to 4. There is one Π group (Π_{S-2}, 1ϕ Natural Circulation with Active PRHR) in which the ratio of its value calculated from the OSU test data to hand calculated value was 20.4. Examination of the calculation for this Π group revealed that the core flow from the test data was 3.5 lb/sec while the calculated core flow was 1.28 lb/sec. Since the core flow is raised to the third power in the equation for Π_{S-2}, the cube of the ratio of the flow rates $(2.7)^3$ is 19.9. Therefore, the difference in the values for Π_{S-2} results from the same order of magnitude difference between the flows rates determined by hand calculation and from the test data as observed in other Π group evaluations. The other Π group whose ratio falls outside the range of 2 to 4 is Π_{S-2}, 2ϕ Natural Circulation. For this parameter, the ratio is 5.9 and is the result of a factor of 2.3 in flow (flow is raised to the second power in this equation).

The same reasoning applied to Π_{S-1} and Π_{S-2}, 1ϕ Natural Circulation with Active Steam Generator, indicates that the flow is higher by a factor of 1.6 since the flow rate is raised to the third power for these Π groups.

3.4.2 Multiloop Scaling

The Π groups for the multiloop, top down analyses with differences between the values calculated by hand and from test data greater than a ratio of 2.0 are shown in Table 3.4-2. There are only four Π groups in the ADS Blowdown Phase and none in the Sump Injection Phase that meet this criterion. The variations in these Π values were caused by differences in the ADS1-3 flow rates.

In the Sump Injection Phase, the flow was nearly constant and the break flow is relatively small with the result that flow rates calculated by hand agreed closely with the experimentally measured flow rates. Therefore, the hand calculation is more accurate during the lower pressure phases of the transient where break flow becomes low, such as IRWST and Sump Injection. It is least accurate during the phases in which the conditions are rapidly changing, as in the initial Natural Circulation and ADS Blowdown Phases and when the break flow is significant.

3.4.3 Bottom-Up Scaling

The Π groups from the Bottom-Up Scaling for which the Π groups calculated by hand differ from those calculated from test data by a factor of 2 are tabulated in Table 3.4-3. There are 7 Π groups that meet this criterion; the ADS Blowdown Phase is the only phase having two Π groups that do not agree. Again, the Sump Injection Phase does not have any Π groups whose values differ by a factor of two.

3.4.4 Conclusions

There is a systematic difference between the Π groups based on hand calculations and those obtained from test data. The ratio of flow rates that resulted in the Π group differences ranges between a factor of 2 and 3. The reason for these differences is the simplifying assumption made to permit calculation of the core flows. In the simplified model, a single closed loop, natural circulation system neglecting the break flow was assumed. The break flow paths were neglected to both simplify the model and to focus on the natural circulation phenomena which was identified as a high ranked phenomena in the PIRT. ***In addtion, the break is a boundary condition, which is a parameter of the test matrix.*** The absence of the break flow in the model resulted in a consistently low calculated flow rate compared to the actual flow measured in the tests. ***Neglecting the break flow in the scaling analysis did not affect other aspects of the facility scaling.*** However, since the same methodology was applied to calculating the Π groups for the AP600 and the test facilities, use of hand calculated Π groups for evaluating the scaling of the test facilities is valid. ***The test data are appropriate for code validation since the breaks were properly scaled in the tests. To ensure that the entire pressure range was adequately investigated, SPES-2 was designed for the high pressure transients and OSU was designed for the low pressure transients.***

Since the Bottom-Up Scaling showed that at least one test facility was scaled within the acceptable range, the test data from the acceptable facility are valid for plant performance code validation. These test data include the transient effects and parallel flows not modeled in the simplified hand calculations and are therefore sufficient for code validation.

The largest variations between the calculated Π groups and those obtained from test data occurred during the early phases of the test during depressurization. During this phase, the conditions are rapidly changing leading to the apparent differences. In quasi-steady operation during the long-term cooling phases, the agreement between the Π groups based on steady-state calculations and the test data agree more closely. Variations in the Π groups during long-term cooling are caused primarily by uncertainties in ADS flows. The uncertainties arise because of the difficulty in

measuring small steam flows and the possibility that the PRHR is condensing some of the steam. The latter effect has been ignored in the analysis.

Since the Bottom-Up Scaling showed that at least one test facility was scaled within the acceptable range, the test data from the acceptable facility are valid for plant performance code validation. These test data include the transient effects and parallel flows not modeled in the simplified hand calculations and are therefore sufficient for code validation.

Table 3.4-1 Single Loop Π Groups with Large[1] Differences Between Test Data and Hand Calculated Values								
		SPES-2			OSU			
Π Group	Equation	Hand Calc	Test Data	Max. Ratio	Hand Calc	Test Data	Max. Ratio	Comments
1ϕ Natural Circulation with Active Steam Generator								
Π_{S-1}	$\dfrac{\left[\dfrac{L_o}{A_o}\right]\dfrac{C_p W_o^3}{\rho_o V_o}}{\beta g \rho_o Q_o \Delta Z_o}$	0.0301	0.1147	3.8	OK	OK		Flow in SPES-2 ~ 60% higher than hand calc.
Π_{S-2}	$\dfrac{\dfrac{R_o}{A_o^2}\dfrac{C_p W_o^3}{2\rho^o}}{\beta g \rho_o Q_o \Delta Z_o}$	1.061	4.048	3.8	OK	OK		Flow in SPES-2 ~ 60% higher than hand calc.
1ϕ Natural Circulation with Active PRHR								
Π_{S-2}	$\dfrac{\left[\dfrac{R_o}{A_o^2}\right]\dfrac{C_p W_o^3}{2\rho_o}}{\beta g \rho_o Q_o \Delta Z_o}$	N.A	N.A		0.59	12.07	20.4	Flow in OSU is factor of 2.7 greater than hand calculated flow. (Flow rate is cubed in Π group)
Π_{S-4}	$\dfrac{W_o C_{p,o} \Delta T_o}{Q_o}$	N.A.	N.A.		1.178	0.435	2.7	

Table 3.4-1	Single Loop Π Groups with Large[1] Differences Between Test Data and Hand Calculated Values (cont.)							
		SPES-2			OSU			
Π Group	Equation	Hand Calc	Test Data	Max. Ratio	Hand Calc	Test Data	Max. Ratio	Comments
2φ Natural Circulation								
$\Pi_{S\text{-}2}$	$\dfrac{\dfrac{W_o^2}{2\bar{\rho}_o}\left(\dfrac{R^2}{A}\right)_o}{g\Delta\rho_o\Delta Z_o}$	0.90	5.35	5.9	0.27	--		Flow in SPES-2 higher than hand calculated value by factor of 2.3
$\Pi_{S\text{-}8}$	$\dfrac{W_o h_o}{Q_o}$	0.231	0.498	2.2	0.443	--		Flow in SPES-2 higher than calculated value by factor of 2.2
ADS1 Injection								
$\Pi_{S\text{-}7}$	$\dfrac{W_o\alpha_{ce}(e_g\rho_g - e_f\rho_f)}{\rho_o Q_o}$	2.360	0.849	2.8	OK	OK		
$\Pi_{S\text{-}10}$	$\dfrac{W_{ADS}C_{v,o}\,\Delta T_o}{Q_o}$	1.045	0.423	2.5	OK	OK		$\Pi_{S\text{-}10}$ and $\Pi_{S\text{-}14}$ are equal since $C_v = C_p$ when most of the mass is liquid.
$\Pi_{S\text{-}14}$	$\dfrac{C_{p,o}\,\Delta T_o\,W_{ADS}}{Q_o}$	1.045	0.423	2.5	OK	OK		ADS flow is lower than hand calculated value in SPES-2 by factor of 2.5.

Table 3.4-1 Single Loop Π Groups with Large[1] Differences Between Test Data and Hand Calculated Values (cont.)								
		SPES-2			OSU			
Π Group	Equation	Hand Calc	Test Data	Max. Ratio	Hand Calc	Test Data	Max. Ratio	Comments
$\Pi_{S\text{-}11}$	$\frac{W_{ADS}\, C_{v,o}}{\beta_o\, Q_o}$	4.46	1.595	2.8	OK	OK		ADS flow in SPES-2 is lower than hand calculated by factor of 2.5.

Table 3.4-1 Single Loop Π Groups with Large[1] Differences Between Test Data and Hand Calculated Values (cont.)								
		SPES-2			OSU			
Π Group	Equation	Hand Calc	Test Data	Max. Ratio	Hand Calc	Test Data	Max. Ratio	Comments
ADS1 and ADS2 Injection								
Π_{S-8}	$\frac{W_{ADS}\, h_{ADS}}{Q_o}$	9.684	3.848	2.5	9.244	4.287	2.2	ADS flow in both SPES-2 and OSU lower by factors of 2.5 and 2.2 than hand calculated value.
Π_{S-7}	$\frac{W_o \alpha_{ce}(e_g \rho_g - e_f \rho_f)}{\rho_o Q_o}$	12.890	5.123	2.5	15.832	7.342	2.2	Core flow in both SPES-2 and OSU lower by same factors as above.
Π_{S-10}	$\frac{W_{ADS} C_{v,o} \Delta T_o}{Q_o}$	4.625	2.034	2.3	3.410	1.333	2.6	
Π_{S-14}	$\frac{W_{ADS} C_{p,o}\, \Delta T_o}{Q_o}$	4.625	2.034	2.3	3.410	1.333	2.6	
Π_{S-11}	$\frac{W_{ADS}\, C_{p,o}}{\beta_o\, Q_o}$	23.791	9.455	2.5	29.716	13.781	2.2	ADS flow is lower in SPES-2 by factor of 2.5 and by factor of 2.2 in OSU.
Π_{S-12}	$\frac{W_{ADS}\, h_{fg,o}}{Q_o\, \rho_{mo}\, V_{fg}}$	0.255	0.1090	2.3	0.1434	0.0425	3.4	ADS flow low in SPES-2 and OSU.
IRWST Injection								

Table 3.4-1 Single Loop Π Groups with Large[1] Differences Between Test Data and Hand Calculated Values (cont.)

Π Group	Equation	SPES-2			OSU			Comments
		Hand Calc	Test Data	Max. Ratio	Hand Calc	Test Data	Max. Ratio	
Π_{S8}	$\frac{X_{ce} W_o h_{fo}}{Q_o}$	0.814	1.905	2.3	OK	OK		Core flow is factor of 2.3 higher in SPES-2 test than calculated value.

Table 3.4-1 Single Loop Π Groups with Large[1] Differences Between Test Data and Hand Calculated Values (cont.)

Π Group	Equation	SPES-2			OSU			Comments
		Hand Calc	Test Data	Max. Ratio	Hand Calc	Test Data	Max. Ratio	
Sump Injection								
Π_{S2}	$\frac{W_o^2 \sum R_{AB}}{\rho_o^2 A_o^2 g L_{gr}}$	N.A.	N.A.		1.230	0.523	2.4	Flow in OSU is lower than hand calculated value by factor of ~ 1.5.

[1] Greater than factor of 2

Note: Π Groups < 0.1 are assumed to be negligible.

Table 3.4-2 Multi-Loop Π Groups with Large[1] Differences Between Test Data and Hand Calculated Values								
Π Group	Equation	SPES-2		Max. Ratio	OSU		Max. Ratio	Comments
		Hand Calc	Test Data		Hand Calc	Test Data		
ADS Blowdown								
Π_{M-1}	$\frac{W_{vess,net}}{W_{ADS\ 1\text{-}3,max}}$	2.4	0.58	4.1	OK	OK		Flows in SPES-2 differ from hand calculated values.
Π_{M-7}	$\frac{W_{ACC,max}\ h_{ACC,max}}{W_{ADS1\text{-}3,max}\ h_{ADS1\text{-}3,max}}$	0.31	0.09	3.3	OK	OK		Flows in SPES-2 differ from hand calculated values.
Π_{M-8}	$\frac{W_{CMT,max}\ h_{CMT,max}}{W_{ADS1\text{-}3,max}\ h_{ADS1\text{-}3,max}}$	0.31	0.13	2.4	0.31	0.63	2.0	Flows in SPES-2 and OSU differ from hand calculated values.
Π_{M-11}	$\frac{Q_c}{W_{ADS1\text{-}3,max}\ h_{ADS1\text{-}3,max}}$	OK	OK		*0.21*	*0.79*	*3.8*	ADS1-3 flow in OSU greater by factor of 3.8 than hand calculated value.
Sump								
	None							

[1] Differences greater than factor of 2

Note: Π Groups with values <0.1 are negligible.

Table 3.4-3 Bottom-Up Π Groups with Large[1] Differences Between Test Data and Hand Calculated Values								
Π Group	Equation	SPES-2		Max. Ratio	OSU		Max. Ratio	Comments
		Hand Calc	Test Data		Hand Calc	Test Data		
Blowdown Phase								
$\Pi_{BR\text{-}1}$ Normalized Break Flow	$\frac{W_B}{W_C}$	0.0094	0.033	3.5	0.0092	0.023	2.5	Flows in both SPES-2 and OSU differ from hand calculated values.
1φ Natural Circulation with Steam Generator								
$\Pi_{BR\text{-}1}$ Normalized Break Flow	$\frac{W_B}{W_C}$	0.24	0.085	2.8	OK	OK		Flows in SPES-2 differ from hand calculated values.
1φ Natural Circulation with PRHR								
$\Pi_{BR\text{-}1}$ Normalized Break Flow	$\frac{W_B}{W_C}$	N/A	N/A		0.46	1.0	2.2	Flows in OSU differ from hand calculated values.

Table 3.4-3	Bottom-Up Π Groups with Large[1] Differences Between Test Data and Hand Calculated Values							
		SPES-2			OSU			
Π Group	Equation	Hand Calc	Test Data	Max. Ratio	Hand Calc	Test Data	Max. Ratio	Comments
ADS Blowdown								
Π_{ADS-1} ADS Critical Flow	$\frac{W_{ADS1}}{W_c}$	0.64	0.25	2.6	OK	OK		Flows in SPES-2 differ from hand calculated values
Π_{BR-1} Normalized Break Flow	$\frac{W_B}{W_c}$	0.46	2.7	5.9	2.2	0.7	3.1	Flows in both SPES-2 and OSU differ from hand calculated values.

Table 3.4-3 Bottom-Up Π Groups with Large[1] Differences Between Test Data and Hand Calculated Values (cont.)

Π Group	Equation	SPES-2		Max. Ratio	OSU		Max. Ratio	Comments
		Hand Calc	Test Data		Hand Calc	Test Data		
IRWST Injection								
Π_{HL-1} Separation at ADS4 tee	$\dfrac{\dfrac{v_g\sqrt{\rho_g}}{\sqrt{g\Delta\rho\ Z_g}}}{5.7\left(\dfrac{L_g}{D}\right)^{3/2}}$	0.069	0.008	8.6	OK	OK		Distortion in SPES-2 results from piping that could be not scaled to the small diameter required for the P/V scaling.
$\Pi_{IRWST-4}$ Gravity draining injection	$\dfrac{R^2/A^2\ W^2_{DVI,o}\ /\ 2_{\rho_{DVI,o}}}{(g\rho\ \Delta Z)_{ref,0}}$	0.69	0.33	2.1	0.66	0.11	6.0	DVI flows are low in SPES-2 by factor of 1.4 and in OSU by a factor of 2.5
[illegible]p								
	None							

(1) Differences greater than factor of 2

Note: Π Groups with values <0.1 are negligible.

Question 440.769F (OITS - 6343)

Inadvertent actuation or malfunction of the CMTs can cause an increase in RCS inventory. The events may lead to an overfill of the pressurizer and possible loss of reactor coolant. The analysis of the inadvertent actuation of the CMTs is performed with the plant initially in Mode 1, full-power condition and is discussed in SSAR 15.5.1. The reactor trip and the PRHR HX actuation are actuated on the Hi-3 pressurizer level trip setpoint. During the event, the CMTs inject cold and borated fluid into the RCS. The injected fluid expands as it is heated in the RCS by the decay heat. The expansion is counteracted by the heat removal from the PRHR HX. Westinghouse stated that the severity of the fluid expansion increases with higher decay heat levels and claimed that the case at full-power (producing a maximum decay heat) bounds the results initiated from conditions below Mode 1. The fluid expansion is controlled by the injection rate, the core decay heat level and the heat removal rate. At shutdown operations, while decay heat levels are lower, heat removal from the PRHR HX is also lower. The staff notes that in the absence of analyses to quantify the total effect of the injection rate, decay heat levels and the heat removal rate from the PRHR HX on the fluid expansion, it is not clear that the full-power case bounds conditions below Mode 1. Westinghouse is requested to analyze the CMT malfunction events at shutdown modes and show that the results are acceptable.

Response:

Inadvertent actuation or malfunction of the CMTs can cause an increase in RCS inventory. The events may lead to an overfill of the pressurizer and possible loss of reactor coolant. During the event, the CMTs inject cold and borated fluid into the RCS. The injected fluid expands as it is heated in the RCS by the decay heat. The expansion is counteracted by the heat removal from the PRHR heat exchanger. The severity of the overfill transient is a function of the magnitude of the decay heat produced, the heat removal capacity of the PRHR heat exchanger and the CMT injection flow rate. The most limiting initial condition for these types of events is from full power conditions because this results in the most decay heat. This response provides the basis for the this conclusion.

The PRHR heat removal capability is a function of the fluid temperature entering the heat exchanger and the flow conditions. Under forced RCS flow conditions at full power normal operating temperatures, the PRHR heat exchanger can remove ~ 10% of rated core power. With full power temperatures and natural circulation flow, the PRHR heat exchanger can remove ~4% of rated power. As the temperature of the fluid entering the PRHR heat exchanger is decreased, the heat removal is decreased. Under natural circulation flow conditions, at 500 °F the PRHR can remove ~1.4% of rated power, at 400 °F the PRHR can remove ~0.8% of rated power and at 350 °F the PRHR can remove on the order of ~0.2% of rated power.

Figure 440.769F-1 shows the initial core decay heat level fraction as a function of the initial total core power level. At an initial total core power level of 100%, the decay heat level would be 7.65% of rated full power. A spurious "S" signal which causes inadvertent actuation of the CMTs and trip of the reactor coolant pumps from full power conditions would result in an increase in the pressurizer level because the decay heat immediately after reactor trip would be ~ 7.65% of rated power, but the

PRHR would only be capable of removing on the order of ~1.4% of rated power. In this case the unremoved decay heat would be absorbed in the reactor coolant and cause an increase in reactor coolant volume.

As the initial power level decreases, the decay heat level decreases proportionately. At a total core power level of 1%, the initial decay heat level is 0.08%. An inadvertent actuation of the CMTs from low power or HZP (i.e. Mode 2) conditions should not result in an overfill transient because the PRHR can remove on the order of 1.4%. In this case the PRHR can remove all of the core decay heat and will have excess capacity that will cause a shrinkage of the reactor coolant fluid. Therefore, based on a comparison of the decay heat levels to PRHR heat removal capacity, at low initial power levels and in the lower operating modes, inadvertent operation of the CMTs, when followed by actuation of the PRHR, will not result in an overfill of the pressurizer. In fact, these scenarios will result in a reduction in pressurizer water volume.

To verify this hypothesis, the following cases were analyzed.

Case 1 Spurious "S" case from 102% power
Case 2 Spurious "S" case from HZP conditions, (545 °F) (Mode 2)
Case 3 Spurious "S" case from 420 °F (Mode 3)
Case 4 Spurious "S" case from 350 °F (Mode 4)

The cases analyze the scenario where a spurious Safeguards ("S") signal causes inadvertent operation of the CMTs. On the "S" signal the reactor is tripped, the PRHR is actuated and the reactor coolant pumps are tripped. For the purpose of maximizing decay heat, Cases 2, 3 and 4 are started from a power level of 1% of rated power. The case from 102% power (Case 1) is included for comparison with the cases at lower modes.

Figure 440.769F-2 shows the pressurizer water volume for the four sensitivity cases. Case 1 shows the pressurizer water level increasing after the CMTs are initiated. In Case 1, the core decay heat immediately after reactor trip is larger than the heat removal capability of the PRHR and therefore the injected CMT fluid absorbs the excess decay heat and expands. In Cases 2 through 4, the pressurizer water volume decreases after the CMTs and the PRHR are actuated. In these cases, although the initial RCS temperatures are lower causing the effective heat removal capability of the PRHR heat exchanger to be lower, the heat removal capability of the PRHR is much larger than the core decay heat produced. Therefore, the net effect is a shrinkage of the reactor coolant fluid even though the CMTs are injecting. Figure 440.769F-3 shows the core and PRHR heat transfer for Case 4. As shown in the figure, although the PRHR heat transfer rate is very low due to the relatively low reactor coolant temperatures, the PRHR heat transfer rate is significantly higher than the heat production in the core.

SSAR Section 15.5.1 presents analyses of the inadvertent operation of the CMTs from full power conditions. The inadvertent operation of the CMTs can be postulated to be due to either a spurious "S" signal or an inadvertent opening of the CMT discharge valves. Both events results in similar consequences with the inadvertent opening of CMT discharge valves scenario being slightly more severe at full power.

In the case of the spurious "S" signal, the PRHR is actuated concurrent with the "S" signal and the reactor coolant pumps are tripped. In the case of the inadvertent opening of the CMT discharge valves, the CMTs injection flow is initially degraded (reduced) because the reactor coolant pumps are operating. The CMTs inject borated water slowly into the reactor coolant causing core power to decrease. Assuming the rod control system is in operation, rods will be withdrawn and core power is returned to match turbine load. During this period pressurizer level increases. When the pressurizer level reaches the high-3 setpoint the reactor is tripped and the PRHR is actuated. In this instance the pressurizer level would then begin decreasing because the PRHR heat removal capability is very large (up to ~10%) when the reactor coolant pumps are operating. The case presented in the SSAR considers a consequential loss of offsite ac power following the trip of the reactor which causes a loss of power to the reactor coolant pumps. When the reactor coolant flow changes from forced flow to natural circulation flow, the CMT flow increases and more importantly the PRHR heat removal capability decreases. The assumption of loss of offsite power following reactor trip causes the inadvertent opening of the CMT discharge valves to be more severe than the spurious "S" signal at full power conditions.

In the lower modes, the turbine/generator is offline and power to plant auxiliaries is supplied by offsite power sources. Consideration of a consequential loss of offsite power is not considered in this case because there is no disruption of the grid. If an inadvertent opening of the CMT discharge valves is postulated in the lower modes, the pressurizer will slowly fill until the high-3 pressurizer level setpoint is exceeded and the PRHR is actuated. Pressurizer level will then decrease at rate greater than that observed in Cases 2 through 4 above because the reactor coolant pumps are still operating and PRHR heat removal capability will be enhanced.

In summary, the most limiting pressurizer overfill scenarios for inadvertent operation of the CMTs occur at full power conditions because the decay heat levels following reactor trip are higher than when the events are postulated to occur in the shutdown modes. In the shutdown modes, the PRHR heat exchanger has sufficient capacity to cause an overall reduction in reactor coolant volume following inadvertent operation of the core CMTs.

SSAR Revision: None

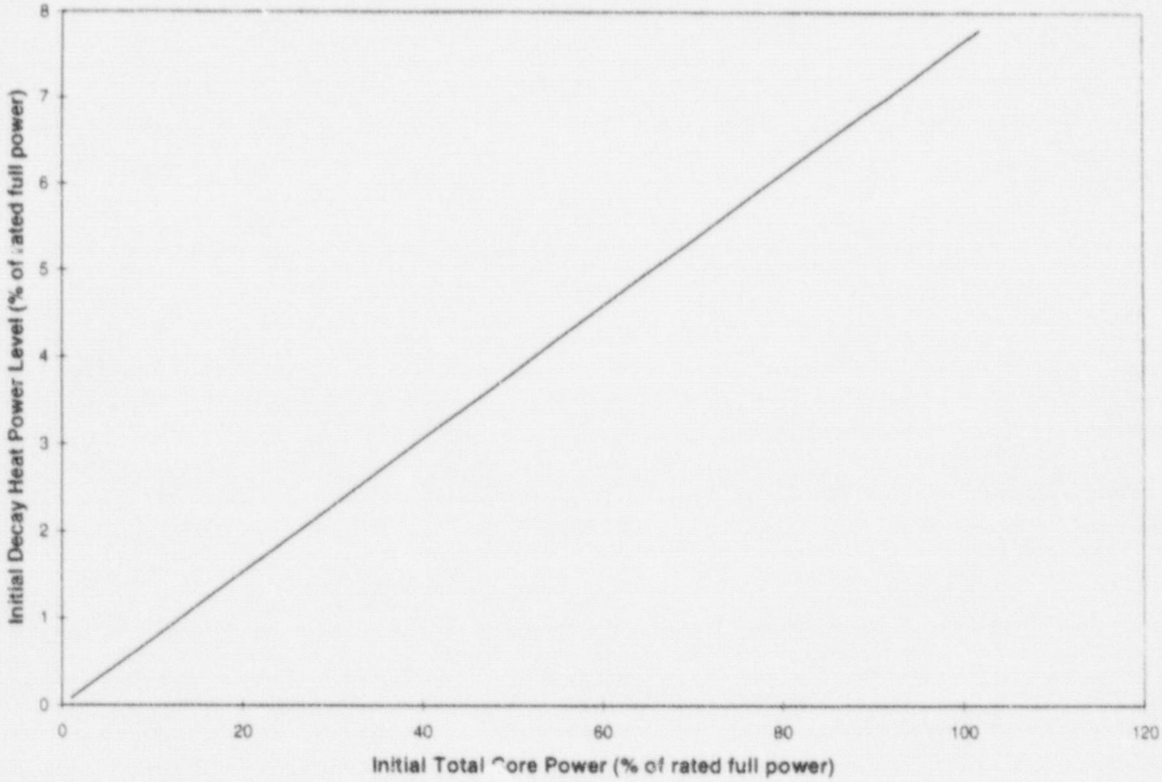

Figure 440.769F-1

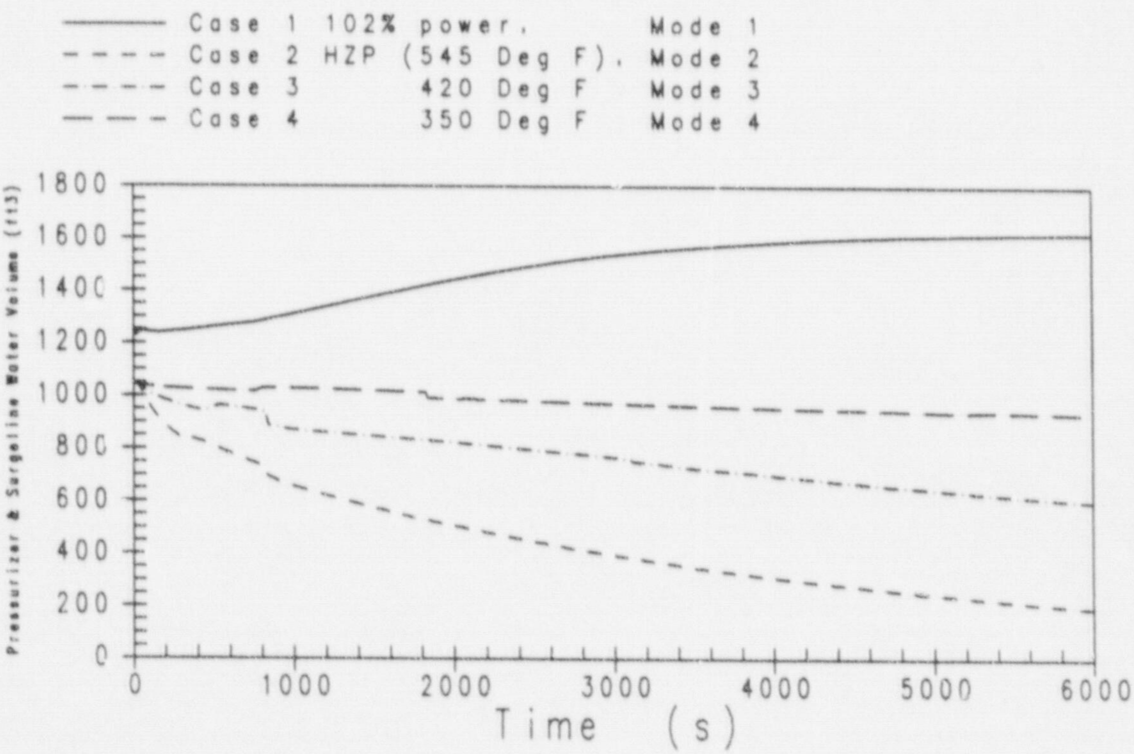

Figure 440.769F-2

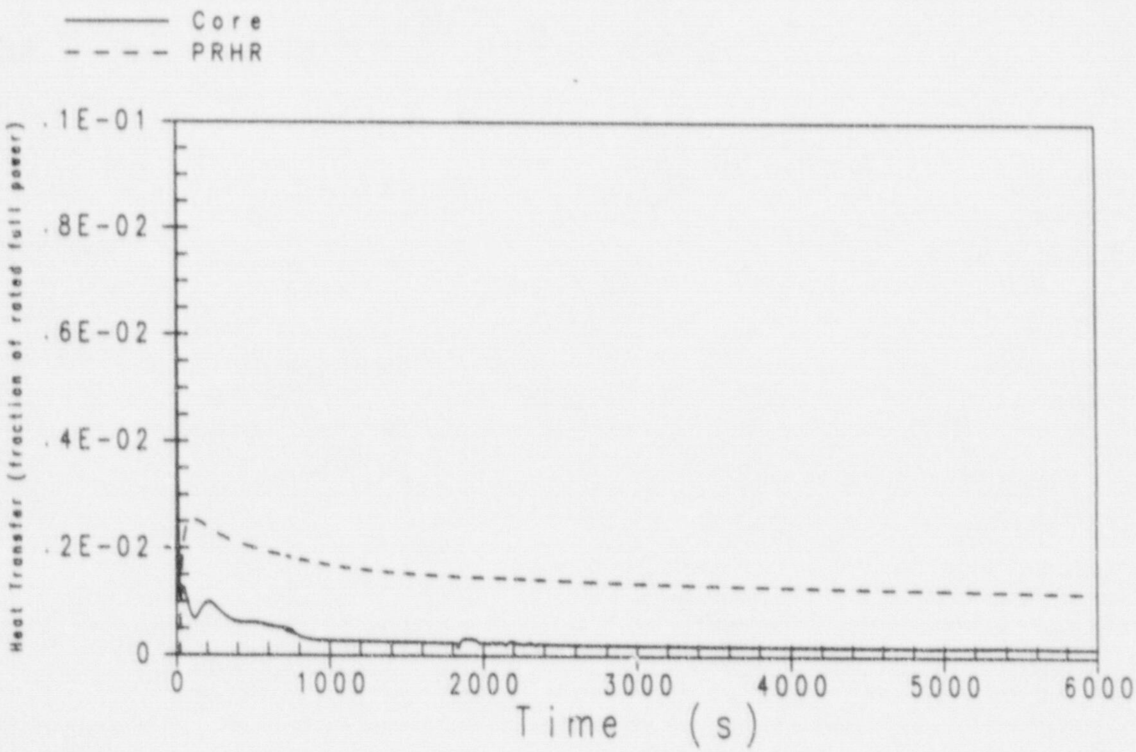

Figure 440.769F-3
Heat Flux for Spurious "S" Case 4 Initiated at 350 °F (Mode 4)

Question 480.1107 (OITS #6376) Revision 1

AP600 IRWST Hydro-Dynamic Loads

(a) In WCAP-13891,"AP600 Automatic Depressurization System Phase A Test Data Report," a floor pressure plot for test A-11, PE-10, page 380, shows a pronounced pressure oscillation beginning approximately 22.70 seconds and decaying quickly to zero by 22.80 seconds. This oscillation appears to be significantly larger, in terms of measured wall pressure, than any of the other tests conducted as shown in WCAP-13891, Table 1 "Test Matrix." Please explain the reason for this oscillation occurring at approximately 22.7 seconds and why the magnitude of this rapidly decaying pulse does not appear on other pressure plots. Also, provide the structural significance of this load on the walls of the AP600.

(b) In WCAP-13891,"AP600 Automatic Depressurization System Phase A Test Data Report," a floor pressure plot for test A-18, PE-10, page 464, does not show the same spike at 22.7 seconds but a much lower and earlier peak occurring at approximately 5 seconds. This would appear to be within the air clearing phase of the quencher phase followed by somewhat steady steam condensation out to 50 seconds. The expanded time scale plot on page 465 of WCAP-13891 provides added insight into the peaks occurring at approximately 5.0 seconds which shows irregular oscillations shifted to the positive pressure and appear to be characteristic of an oscillating air bubble. The negative portion of the curve appears jagged, irregular and uncharacteristic of an air bubble rising to the surface. Please explain what phase the quencher is operating in (i.e. air clearing or unsteady steam condensation) and the apparent difference with essentially the same test conditions except for nominal temperature as test A11 as shown in WCAP-13891, Table 1 "Test Matrix."

Response:

The Phase A portion of the ADS testing was performed to obtain bounding data for guidance in the preliminary design of the IRWST and related structures and to confirm the satisfactory operation of the prototype sparger. However, these tests contained many non-prototypicalities including: the rate at which flow was initiated was not consistent with the AP600 ADS valve opening times, the blowdown fluid was only steam and did not include two-phase fluid, the flow rates achieved were typically larger than the actual AP600 volumetric flow rates, and the sparger was located very close to the bottom of the quench tank. For these reasons the data from this Phase A portion of the ADS testing program was not directly used in developing the sparger generated forcing functions used to establish the loads on the IRWST structure and submerged equipment within the IRWST, and can be eliminated from consideration for NRC review as part of the AP600 certification. It is noted however that the more prototypic data from the subsequent Phase B ADS testing, was compared to portions of the Phase A data to aid our understanding of the hydrodynamic pressure pulses that occur during ADS operation. The IRWST hydrodynamic load analysis document which is to be submitted in response to RAI 480.1105 (OITS #6374) will specify the ADS test data used to develop the appropriate AP600 loads.

Responses to the specific questions asked about instrument PE-10, Test Run A-11; and Test A-18 are included below for completeness:

(a) The pronounced oscillations beginning at 22.7 seconds recorded on the PE-10 instrument channel in ADS Phase A test A-11 are not actual pressure pulses occurring in the test quench tank due to hydrodynamic forces associated with the ADS blowdown/sparger operation. The recorded pulses are due to the introduction of signal noise into the analog data collection electronic equipment used in this early series of ADS tests, which includes the cabling, signal amplifiers/conditioners, FM tape recorder(s), etc. This is evidenced by the fact that the initiating pulse in test A-11 is very rapid and reaches the full scale of the instrument and then followed by decaying pulses at 100 hertz which is just 2 times the ac electrical power frequency at the VAPORE test facility. Note the very symmetrical shape of the oscillations and constant decay of the oscillation amplitude. In addition, the fact that this very large magnitude pulse and subsequent decay are not simultaneously measured by any of the other pressure instruments in the test tank, the fact that pulses of this type are not observed to occur regularly or in response to specific test run flow conditions, and the fact that these pulses were not observed in the Phase B ADS testing (performed with a high speed digital data acquisition system and revised pressure sensors/cabling) are further evidence that the pulse is spurious.

(b) Based on the plots of temperature vs. time of the fluid in the sparger arms for ADS Phase A test A-18, provided on pages 614 and 615; air-only clearing occurs from 0 to 5 seconds, followed by steam and air flow from the sparger into the quench tank ~~is initiated at~~ from ~5 to 8 seconds. followed by steam only flow which ~~and~~ reaches a "quasi-steady state" prior to 10 seconds. From 10 to 20 seconds the fluid temperature in the sparger arms continues to increase in response to the increasing ADS blowdown flow rate (increasing sparger arm pressure) which peaks at ~20 seconds. Therefore the 5 to 8 second time period is best described as the unsteady steam condensation combined with a decreasing air concentration. The noted shift of the pressure trace during this short time period is consistent with the pressure traces for other Phase A tests performed with the quench tank water initially at 180°F. As noted above, the Phase A tests runs were not prototypic in that the ADS blowdown was initiated at too fast a rate. This resulted in much higher initial pressure pulses than measured during Phase B testing where prototypic ADS valves were opened to initiate flow. Therefore the short term high pressure pulses observed in Test A-18 are not considered to be prototypic. Tests A-11 and A-18 provide a good comparison of the condensation oscillations that occur in cold water versus 180°F, after quasi-steady state conditions are achieved. ~~Comparisons between the loads that occur during this time period for tests A-11, A-18, and A-19 indicate that the initial quench tank water temperature does have a significant impact on both the amplitude, frequency, and shape of the measured pressure pulses.~~

SSAR Revision: None

Question 720.423F (OITS - 6135)

In meeting the RTNSS criteria, credit was taken for external reactor vessel cooling (ERVC) as a strategy for retaining molten core debris in-vessel. This results in the majority of core melt accidents (~90 percent) being arrested in-vessel, thereby avoiding RPV failure and associated containment challenges from ex-vessel phenomena. Successful RCS depressurization and reactor cavity flooding are prerequisites for ERVC, and credit for these aspects of ERVC in the focussed PRA is appropriate since both functions are fulfilled by safety-related systems. However, the nonsafety-related RPV thermal insulation system is also required for successful ERVC. The thermal insulation system limits thermal losses during normal operations, but provides an engineered pathway for supplying water cooling to the vessel and venting steam from the reactor cavity during severe accidents. Attributes of the system include specific RPV/insulation clearances and water/steam flow areas based on scaled tests, integral ball-and-cage check valves and buoyant steam vent dampers which change position during flood-up of the reactor cavity, and insulation panel and support members designed to withstand the hydrodynamic loads associated with ERVC.

If credit for ERVC is reduced, large release frequency and CCFP would increase proportionally since all RPV breaches are assumed to lead to early containment failure in the PRA. Under the most limiting assumption of no credit for ERVC, the large release frequency would approach the core melt frequency and CCFP would approach 1.0. In view of the reliance on ERVC to meet the Commission's large release frequency goals, the staff will require an appropriate level of regulatory oversight of the RPV thermal insulation system. This oversight should provide reasonable assurance that the as-built insulation system conforms with design specifications contained in Chapter 39 of the PRA, and that the operability of the system is confirmed through periodic surveillance.

The RPV insulation design description and functional requirements are not currently included in the SSAR, ITAAC, or reliability assurance program. The design description and functional requirements for the RPV insulation should be added to the SSAR, and important criteria associated with the insulation design should be incorporated into the ITAAC, including information related to the necessary clearances/flow areas, and the check valves and steam vent dampers. The system should be included as a risk-significant SSC in the reliability assurance program, and reliability/availability controls and goals should be provided, consistent with maintenance rule guidelines, to assure that operability of the system and moving parts is maintained.

Westinghouse Response (Revision 1):

Functional requirements for the reactor vessel insulation was incorporated in section 5.3.5 of Revision 14 of the AP600 SSAR. Based on discussions with the NRC staff, more information was requested to be included in the SSAR. SSAR Section 5.3.5 is modified to include the design bases and design description for the reactor vessel insulation and is attached. In addition, the reactor vessel insulation is included as a risk-significant SSC in the reliability assurance program as shown in the proposed revision to SSAR section 17.4. The AP600 Certified Design Material is also revised to include appropriate ITAACs for the reactor vessel insulation per the response to RAI 720.442F.

SSAR Section 5.3.5 is further revised based on discussions held with the staff at the January 22, 1998 chapter closeout meeting.

SSAR Revision:

Revised SSAR Sections 5.3.5 and 17.4 attached. See the response to RAI 720.442F for changes to the Certified Design Material.

5.3.5 Reactor Vessel Insulation

5.3.5.1 Reactor Vessel Insulation Design Bases

Reactor vessel insulation is provided to minimize heat losses from the primary system. Nonsafety-related reflective insulation similar to that in use in current pressurized water reactors is utilized. The AP600 reactor vessel insulation contains design features to promote in-vessel retention following severe accidents. In the unlikely event of a beyond design basis accident, the reactor cavity is flooded with water, and the reactor vessel insulation allows heat removal from core debris via boiling on the outside surface of the reactor vessel. The reactor vessel insulation permits a water layer next to the reactor vessel to promote heat transfer from the reactor vessel. This is accomplished by providing:

- A means of allowing water free access to the region between the reactor vessel and insulation.
- A means to allow steam generated by water contact with the reactor vessel to escape from the region surrounding the reactor vessel.
- A support frame to prevent the insulation panels from breaking free and blocking water from cooling the reactor vessel exterior surface.

The reactor vessel insulation and its supports are designed to withstand bounding pressure differentials across the reactor vessel insulation panels during the period that the reactor vessel is externally flooded with water and the core retained in the reactor vessel through heat removal from the vessel wall accomplished by the water. This is accomplished by providing a minimum flow area of 7.5 ft^2 in the portions of the flow paths required to vent steam. The flow path from the reactor loop compartment to the reactor cavity provides an open flow path for water to flood the reactor cavity. The reactor vessel insulation inlet assembles are designed to minimize the pressure drop during ex-vessel cooling to permit water to cool the vessel.

5.3.5.2 Description of Insulation

A schematic of the reactor vessel, the vessel insulation and the reactor cavity is shown in Figure 5.3-7. The insulation is mounted on a structural frame that is supported from the wall of the reactor cavity. The vertical insulation panels are designed to have a minimum gap between the insulation and reactor vessel not less than 2 inches ~~under static load conditions associated with containment floodup~~ when subjected to the dynamic loads in the direction towards the vessel that result during ex-vessel cooling. A nominal gap (with no deflection) of more than twice the minimum gap is provided.

The conical design of the bottom portion of the vessel insulation is constructed of flat panels. This provides a single point of contact with the spherical portion of the vessel in the event that an insulation panel becomes dislodged. This prevents hot spots from developing on the reactor vessel and permits sufficient flow to maintain in-vessel retention. The nominal gap

720.423F-3

between the conical portion of the insulation and the spherical portion of the reactor vessel is not less than 9 inches.

The structural frame supporting the insulation is designed to withstand the bounding severe accident loads without exceeding deflection criteria. The fasteners holding the insulation panels to the frame are also designed for these loads.

At the bottom of the insulation are water inlet assemblies. Each water inlet assembly is normally closed to prevent an air circulation path through the vessel insulation. The inlet assemblies are self-actuating passive devices. The inlet assemblies open when the cavity is filled with water. This permits ingress of water during a severe accident, while preventing excessive heat loss during normal operation.

The total flow area of the water inlet assemblies have sufficient margin to preclude significant pressure drop during ex-vessel cooling during a severe accident. The minimum total flow area for the water inlets assemblies is 6 ft^2. Due to the relatively low approach velocities in the flow paths leading to the reactor cavity, and due to the relatively large minimum flow area through each water inlet assembly, with an area of at least 7 in^2 ~~(≥ 7 in²)~~, the water inlet assemblies are not susceptible to clogging from debris inside containment.

Near the top of the lower insulation segment are steam vent dampers. These dampers are normally closed to prevent reactor vessel heat loss, and a small buildup of steam pressure under the insulation will cause them to open to the vent position. The steam vent dampers are passive, self-actuated devices and will operate when steam is generated under the insulation with the cavity filled with water.

~~In-vessel retention requires a flow path from the reactor coolant loop compartments to the reactor cavity. The path from the loop compartments to the reactor cavity is open, and free from obstructions that could block water from flooding the cavity during an accident. Doors in this flow path that could preclude a minimum flow area of 6 ft² such as the door between the reactor coolant drain tank room and the reactor cavity are required to open to permit water to flood the reactor cavity compartment.~~

Extensive maintenance of the vessel insulation is not normally required. Periodic verification that the vessel insulation moving parts can be performed during refueling outages.

5.3.5.3 Description of External Vessel Cooling Flooded Compartments

Ex-vessel cooling during a severe accident is provided by flooding the reactor coolant system loop compartment including a vertical access tunnel, the reactor coolant drain tank room, and the reactor cavity. Water from these compartments replenishes the water that comes in contact with the reactor vessel and is boiled and vented to containment. The opening between the vertical access tunnel and the reactor coolant drain tank room is approximately 100 ft^2. The opening between the reactor coolant drain tank room and the reactor cavity is approximately 48 ft^2. Figure 5.3-8 depicts the flooded compartments that provide the water for ex-vessel cooling. The opening between the reactor coolant drain tank room and the

720.423R-4

reactor cavity is free from obstruction such that it does not preclude a minimum flow area of 6 ft^2 to permit water to flood the reactor cavity compartment.

5.3.5.4 Determination of Forces on Insulation and Support System

The expected forces that may be expected in the reactor cavity region of the AP600 plant during a core damage accident in which the core has relocated to the lower head and the reactor cavity is reflooded have been conservatively established based on data from the ULPU test program (Reference 5). The particular configuration (Configuration III) reviewed closely models the full-scale AP600 geometry of water in the region near the reactor vessel, between the reactor vessel and the reactor vessel insulation. The ULPU tests provide data on the pressure generated in the region between the reactor vessel and reactor vessel insulation. These data, along with observations and conclusions from heat transfer studies, are used to develop the functional requirements with respect to in-vessel retention for the reactor vessel insulation and support system. Interpretation of data collected from ULPU Configuration III experiments in conjunction with the static head of water that would be present in the AP600 is used to estimate forces acting on the rigid sections of insulation. Further evaluation of the forces on the reactor vessel insulation and supports is provided in the AP600 Probabilistic Risk Assessment.

5.3.5.5 Design Evaluation

A structural analysis of the AP600 reactor cavity insulation system demonstrates that it meets the functional requirements discussed above. The analysis encompassed the insulation and support system and included a determination of the stresses in support members, bolts, insulation panels and welds, as well as deflection of support members and insulation panels.

The results of the analyses show that the insulation is able to meet its functional requirements. The reactor vessel insulation provides an engineered pathway for water-cooling the vessel and for venting steam from the reactor cavity.

The reactor vessel insulation is purchased equipment. The purchase specification for the reactor vessel insulation will require confirmatory static load analyses.

5.3.6 Combined License Information

5.3.6.1 Pressure-Temperature Limit Curves

The pressure-temp. curves shown in Figures 5.3-2 and 5.3-3 are generic curves for AP600 reactor vessel design, and they are the limiting curves based on copper and nickel material composition. However, for a specific AP600, these curves will be plotted based on material composition of copper and nickel. Use of plant-specific curves will be addressed by the Combined License applicant during procurement of the reactor vessel.

720.423F-5

5.3.6.2 Reactor Vessel Materials Surveillance Program

The Combined License applicant will address a reactor vessel reactor material surveillance program based on subsection 5.3.2.6.

5.3.6.3 Reactor Vessel Materials Properties Verification

The Combined License applicant will address verification of plant-specific belt line material properties consistent with the requirements in subsection 5.3.3.1 and Tables 5.3-1 and 5.3-3.

5.3.6.4 Reactor Vessel Insulation

The Combined License applicant will address verification that the reactor vessel insulation is consistent with the design bases established for in-vessel retention.

5.3.7 References

1. ASTM E-185-82, Standard Practice for Conducting Surveillance Tests for Light-Water Cooled Nuclear Power Reactor Vessels."

2. Soltesz, R. G., et al., "Nuclear Rocket Shielding Methods, Modification, Updating, and Input Data Preparation, Volume 5 -Two-Dimensional Discrete Ordinates Techniques," WANL-PR-(LL)-034, August 1970.

3. SAILOR RSIC Data Library Collection DLC-76, "Coupled, Self-Shielded, 47 Neutron, 20 Gamma-Ray, P3, Cross Section Library for Light Water Reactors."

4. NRC Policy Issue, "Pressurized Thermal Shock," SECY-82-465, November 23, 1982.

5. Theofanous, T.G., et al., "In-Vessel Coolability and Retention of a Core Melt," DOE/ID-10460, July 1995.

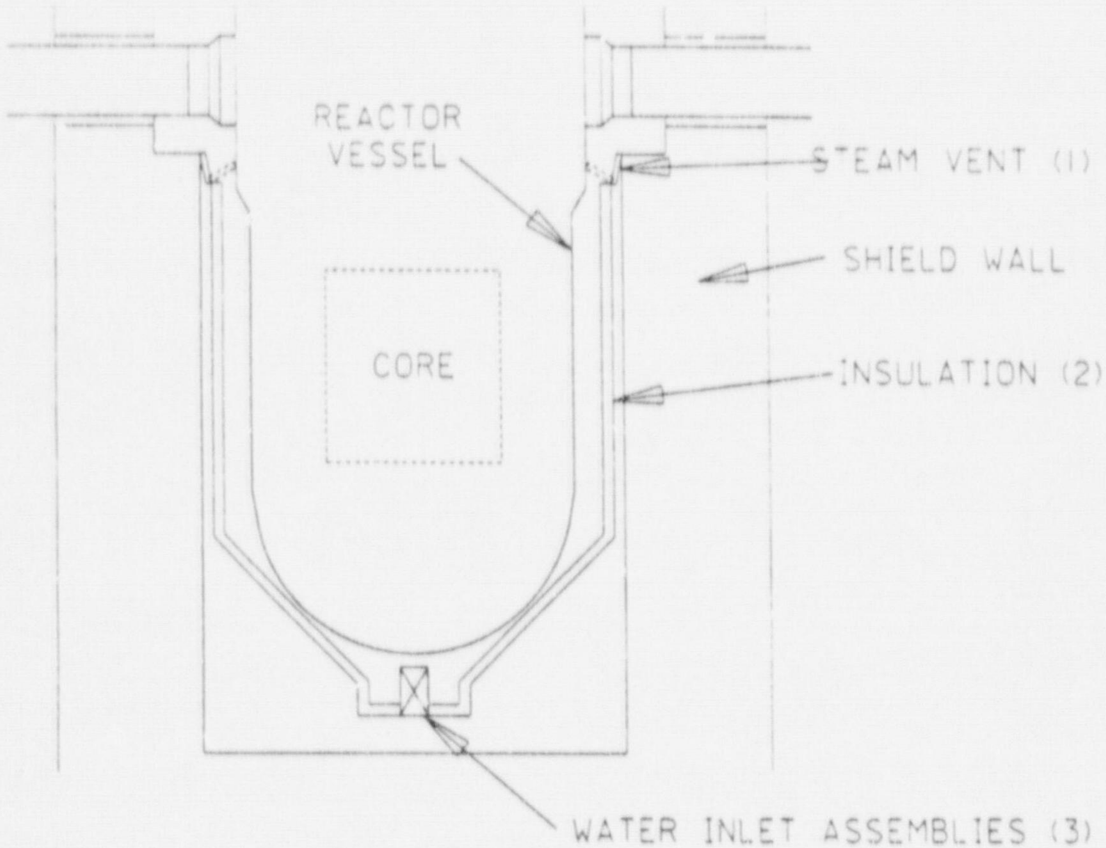

(1) - Minimum steam vent flow area provided in subsection 5.3.5.1
(2) - Minimum gap between insulation and vessel insulation provided in subsection 5.3.5.2
(3) - Minimum flow area provided in subsection 5.3.5.2

Figure 5.3-7

Schematic of Reactor Vessel Insulation

720.423F-7

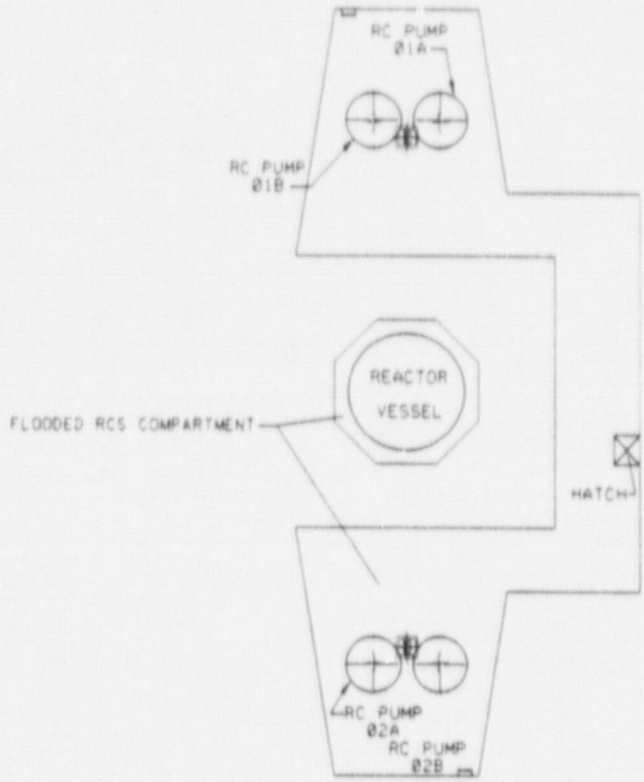

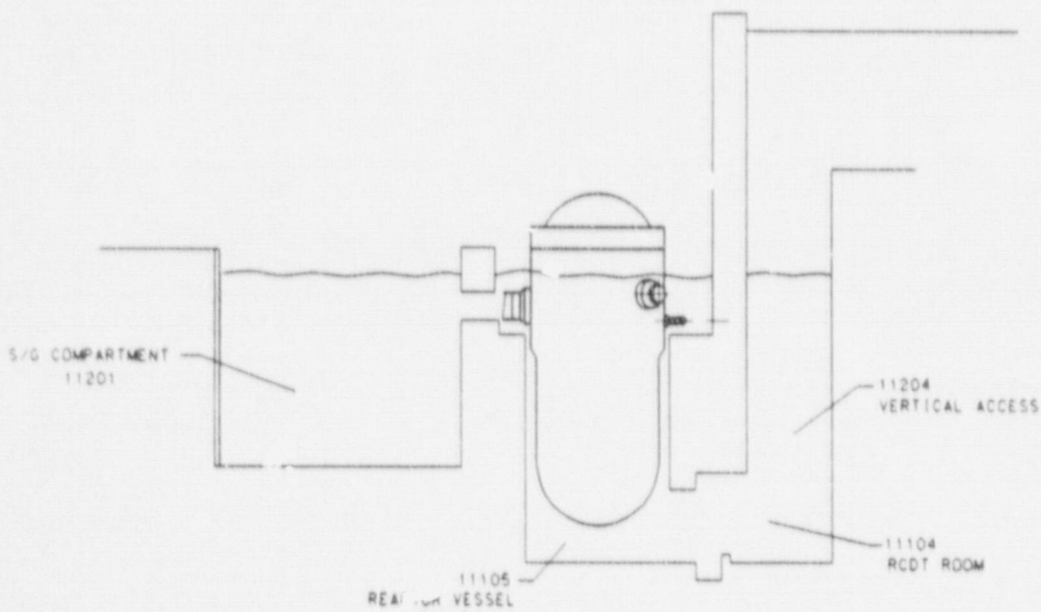

Figure 5.3-8
RCS Flooded Compartments During Ex-Vessel Cooling

726-423F-8

Table 17.4-1 (Sheet 7 of 9)

RISK-SIGNIFICANT SSCs WITHIN THE SCOPE OF D-RAP

System, Structure, or Component (SSC)[1]	Rationale[2]	Insights and Assumptions
System: Reactor Coolant System (RCS)		
ADS Stages 1/2/3 Motor-Operated Valves	EP, L2	The ADS provides a controlled depressurization of the RCS following LOCAs to allow core cooling from the accumulator, IRWST injection, and containment recirculation. The ADS provides "bleed" capability for feed/bleed cooling of the core. The ADS also provides depressurization of the RCS to prevent a high-pressure core melt sequence.
ADS 4th Stage Squib Valves	RAW/CCF	The ADS provides a controlled depressurization of the RCS following LOCAs to allow core cooling from the accumulator, IRWST injection, and containment recirculation. The ADS provides "bleed" capability for feed/bleed cooling of the core. The ADS also provides depressurization of the RCS to prevent a high-pressure core melt sequence.
Pressurizer Safety Valves	EP	These valves provide overpressure protection of the RCS.
Reactor Vessel Insulation Water Inlet and Steam Vent Devices	EP	These devices provide an engineered flow path to promote in-vessel retention of the core in a severe accident.
System: Normal Residual Heat Removal System (RNS)		
RNS Pumps	EP	These pumps provide shutdown cooling of the RCS. They also provide an alternate RCS lower pressure injection capability following actuation of the ADS. The operation of these pumps is RTNSS-important during shutdown reduced-inventory conditions. RNS valve realignment is not required for reduced-inventory conditions.
RNS Motor-Operated Valves	RRW/FVW	These MOVs align a flowpath for nonsafety-related makeup to the RCS following ADS operation.
System: Spent Fuel Cooling System (SFS)		
SFS Pumps	EP	These pumps provide flow to the heat exchangers for removal of the design basis heat load.

720.423F-9